Effects of long-wavelength Klebanoff modes on boundary-layer instability

By Xuesong Wu† AND Meelan Choudhari‡

1. Introduction

It is known that low-frequency components of three-dimensional vortical disturbances in the free stream can be entrained into the boundary layer due to the nonparallel flow effect, producing significant distortion in the form of alternate thickening and thinning of the layer in the spanwise direction. This observation goes back to Dryden (1936) and Taylor (1939) who, in fact, suggested that the entrained vortex motion, rather than the Tollmien-Schlichting (T-S) instability, was the cause of transition to turbulence. The dispute continued until the experiments of Schubauer and Skramstad (1948), which were conducted by minimizing the free-stream perturbations, fully validated the instability theory of Tollmien (1929) and Schlichting (1933). Since then, most research efforts have focused on transition at low levels of free-stream turbulence.

There has also been a significant amount of research on transition at moderate to high free-stream turbulence levels, primarily because of its relevance to turbomachinery flows. This has led to renewed interest in the findings of Dryden (1936) and Taylor (1939). Recent experimental studies (see e.g. Kendall 1985, Westin *et al.* 1994, Matsubara & Alfredsson 2001, and the references therein) show that the boundary layer filters out the high-frequency components of free-stream turbulence, while amplifying the low-frequency parts of the signature. The distortion within the boundary layer is dominated by streamwise velocity fluctuations, which are manifested in the form of longitudinal vortices or streaks. These streaks are now referred to as Klebanoff modes, in recognition of the contribution of Klebanoff (1971). In this paper, we shall refer to them as Klebanoff distortions or fluctuations, so as to avoid possible confusion when genuine instability modes are being discussed.

The boundary-layer response to small-amplitude unsteady vortical disturbances was calculated by Gulyaev *et al.* (1989) and Choudhari (1996) using linearized unsteady boundary-layer equations. Leib *et al.* (1999) pointed out that this approach is restricted to the region relatively close to the leading edge where the spanwise length scale of the perturbation is much larger than the local boundary-layer thickness. The continued growth of the perturbation amplitude and boundary-layer thickness implies that nonlinearity and cross-flow ellipticity will become significant sufficiently farther downstream, at which point the flow must be governed by boundary-*region* equations. For further work in the context of boundary-region equations, the reader is referred to the papers by Wundrow & Goldstein (2001), Goldstein & Wundrow (1998) and other references therein.

Direct laboratory investigations of the transition process in the presence of Klebanoff fluctuations have been made by a number of investigators. At moderate levels of free-stream turbulence, Arnal & Juillen (1978) and Kendall (1990) have observed intermittent appearance of wave packets inside the boundary layer. While their exact origin remains unclear, a series of experiments conducted by Kendall (1991, 1998) has helped reveal

† Permanent address: Department of Mathematics, Imperial College, UK
‡ NASA Langley Research Center, Hampton, VA

some unusual attributes of these wavepackets. First, they appear only when the free-stream turbulence exceeds a threshold amplitude of about 0.1%. Second, their growth rates are considerably larger than those of the T-S waves, being also dependent on the turbulence level. Third, the frequencies of these waves are significantly higher than those of T-S instability. Finally, these packets are more confined laterally, spreading rather slowly in the spanwise direction as they propagate downstream. Thus far, there has been no physical explanation for the above features. However, the present findings will shed some new lights on these observations.

Rather than studying naturally-occurring wavepackets, Watmuff (1997) used a harmonic point source to generate spanwise-localized wavetrains in a controlled fashion. He found that even a weak Klebanoff perturbation can induce severe distortions of the higher-frequency wavetrain, such that any comparison with calculations that do not account for the presence of Klebanoff modes becomes almost meaningless.

In addition to investigating the role of conventional T-S waves during transition in the presence of moderate free-stream turbulence, it is also important to examine alternative instability mechanisms. Streak instability, in particular, has attracted much attention in recent years. Matsubara, Bakchinov & Alfredsson (2000) reported that streaks or Klebanoff modes are unstable, and this can lead to a meandering and oscillation of the streaks and an eventual breakdown into turbulent spots.

In an effort to understand streak breakdown, Andersson *et al.* (2001) modeled the streak structure by a steady, spanwise-periodic distortion to a Blasius boundary layer. An inviscid stability analysis based on Floquet theory suggested that the streaks become unstable only when the amplitude of the associated streamwise velocity perturbation exceeds approximately 26% of the free-stream velocity. This estimate is perhaps too high to be representative of typical Klebanoff distortion in natural disturbance environments. The present theory, however, suggests that the unsteadiness of the Klebanoff distortion (even if at rather low frequencies) may exert a significant effect on the resulting high-frequency secondary instabilities (see §2.2).

Direct numerical simulations of transition due to high free-stream turbulence were performed first by Rai & Moin (1993), and more recently by Jacobs & Durbin (2001). The latter found that the boundary-layer response to free-stream turbulence was indeed dominated by low-frequency streaks. However, these streaks appeared to be fairly stable and it was only after they had lifted up to the outer part of the boundary layer to form a 'backward jet' that the breakdown to turbulent spots occurred.

In this paper, we investigate the instability of a Blasius boundary layer perturbed by Klebanoff distortions. Our main interest will be in relatively small-amplitude distortions, which are not atypical of many experimental situations. As in Wu & Luo (2001, referred to as I hereafter), we shall address two issues: (a) how the T-S instability, which operates in the absence of any distortion, is modified by a weak Klebanoff distortion, and (b) whether or not a weak distortion can induce a predominantly-inviscid instability. An asymptotic approach based on the high-Reynolds-number assumption is used, aimed at a systematic and consistent treatment of both the Klebanoff fluctuation and the secondary instability of the resultant perturbed flow. To make analytical progress, we also assume that the spanwise length scale of the Klebanoff distortion is larger than the thickness of the boundary layer. While the assumptions made will, no doubt, restrict the validity of the conclusions obtained, we believe that the analytical simplicity of this approach provides extra insights that might not have been easily apparent using a less restrictive, but primarily numerical, approach.

2. Formulation

Consider the two-dimensional incompressible boundary layer due to a uniform flow with velocity U_∞ past a semi-infinite flat plate. Superimposed on the incoming stream is a small-amplitude, three-dimensional vortical disturbance (i.e., a *gust*) that is advected at the free-stream speed. For simplicity, we assume that the gust is harmonic in time, with a frequency of $k_1 U_\infty/\Lambda$, where k_1 denotes the non-dimensional frequency parameter and Λ represents the dimensional length scale of the gust in the spanwise direction.

The flow is to be described in the Cartesian coordinate system (x, y, Z), with its origin at the plate leading edge. Here, x, y and Z denote the streamwise, normal, and spanwise coordinates nondimensionalized with respect to Λ. The time variable t is normalized by Λ/U_∞ and the velocity components (u, v, w) and pressure p are normalized by U_∞ and ρU_∞^2, respectively, where ρ denotes the fluid density. The Reynolds number $R_\Lambda \equiv U_\infty \Lambda/\nu$ is assumed to be a large parameter throughout this analysis (i.e., $R_\Lambda \gg 1$).

The streamwise and normal velocity components of the Blasius flow are given by

$$(U_B, V_B) = \left\{ F'(\eta),\ (2xR_\Lambda)^{-\frac{1}{2}}(\eta F' - F) \right\} ,$$

where $\eta = R_\Lambda^{1/2} y/\sqrt{2x}$ and $F(\eta)$ satisfies the Blasius boundary-value problem

$$F''' + FF'' = 0 , \quad \text{with} \quad F(0) = F'(0) = 0; \quad F'(\infty) = 1 . \tag{2.1}$$

2.1. *Flow distortion associated with Klebanoff modes*

The boundary-layer response to a three-dimensional convected gust was analyzed by Gulyaev *et al.* (1989), Choudhari (1996) and Leib *et al.* (1999). Similar to their work, the velocity field of the disturbance superimposed on the oncoming flow has the form

$$\mathbf{u}_\infty = \epsilon_D \Big(\hat{u}_\infty B'(Z), \hat{v}_\infty B'(Z), \hat{w}_\infty B(Z) \Big) \, \mathrm{e}^{\mathrm{i}\, k_1 (x-t) + \mathrm{i}\, k_2 y} , \tag{2.2}$$

where ϵ_D represents the gust amplitude, and k_1 and k_2 denote the streamwise and transverse wavenumbers, respectively. We assume that $k_1,\ k_2 \ll 1$ so that $\hat{w}_\infty \ll \hat{u}_\infty,\ \hat{v}_\infty$ $(= O(1))$. Note that we now allow for a general spanwise dependence of the gust via the arbitrary function $B(Z)$.

The inviscid solution can be written as (Leib *et al.* 1999)

$$\mathbf{u}_D = \epsilon_D [\mathbf{u}_\infty + \bigtriangledown \phi] \tag{2.3}$$

where ϕ denotes the potential. To the required order, ϕ is governed by the boundary value problem

$$\bigtriangledown^2 \phi = 0 , \tag{2.4}$$

$$\left.\begin{aligned} &\bigtriangledown \phi \to 0 \quad \text{as} \quad y \to \infty ; \\ &\phi(x,0) = 0 \quad (x<0), \quad \phi_y(x,0) = -\hat{v}_\infty B'(Z)\, \mathrm{e}^{\mathrm{i}\, k_1 (x-t)} \qquad (x>0). \end{aligned}\right\} \tag{2.5}$$

The full solution to Eqs. (2.4)-(2.5) can be found by the standard Wiener-Hopf technique. However, for the purpose of stability analysis, we confine ourselves to the region $x \gg 1$ and $k_1 \ll 1$, such that $k_1 x = O(1)$. The inviscid solution under these conditions can be obtained by neglecting the x-derivative term in Eq. (2.4) and solving the resultant two-dimensional Laplace equation in the half-space $y > 0$. This yields the slip-velocity components in the streamwise and spanwise directions

$$u_s \approx \hat{u}_\infty, \quad w_s \approx \hat{v}_\infty \frac{\partial}{\partial Z} \int_{-\infty}^{\infty} \frac{B(\zeta)}{\zeta - Z} \, \mathrm{d}\, \zeta . \tag{2.6}$$

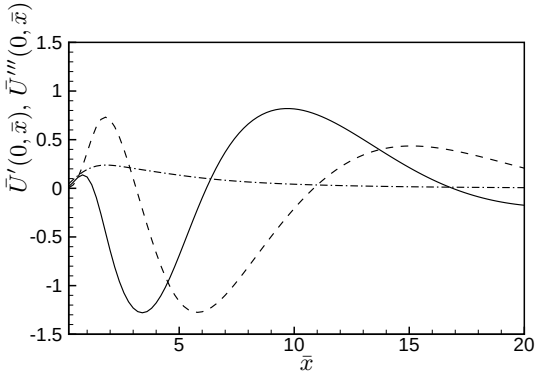

FIGURE 1. Variation of $U'''(0,\bar{x})$ (——— real part, - - - - imaginary part) and $|U'(0,\bar{x})|$ ($-\cdot--\cdot-$) with $\bar{x}$.

The distortion within the boundary layer is a small perturbation to the Blasius flow, and its leading-order solution takes the form

$$(\tilde{U},\tilde{V},\tilde{W}) = \Big[-\frac{w_s'(Z)}{k_1}\bar{U}, -\frac{w_s'(Z)}{k_1}\bar{V}, w_s(Z)\bar{W}\Big]\,\mathrm{e}^{-\,\mathrm{i}\,\bar{t}} + c.c. + \ldots\ . \tag{2.7}$$

where we put $\bar{x} = k_1 x$ and $\bar{t} = k_1 t$. The functions $(\bar{U},\bar{V},\bar{W})$ are governed by the linearized unsteady boundary-layer equations (Leib *et al.* 1999)

$$\frac{\partial\bar{U}}{\partial\bar{x}} - \frac{\eta}{2\bar{x}}\frac{\partial\bar{U}}{\partial\eta} + \frac{\partial\bar{V}}{\partial\eta} + \bar{W} = 0\ , \tag{2.8}$$

$$-\,\mathrm{i}\,\bar{U} + F'\frac{\partial\bar{U}}{\partial\bar{x}} - \frac{F}{2\bar{x}}\frac{\partial\bar{U}}{\partial\eta} - \frac{\eta F''}{2\bar{x}}\bar{U} + F''\bar{V} = \frac{1}{2\bar{x}}\frac{\partial^2\bar{U}}{\partial\eta^2}\ , \tag{2.9}$$

$$-\,\mathrm{i}\,\bar{W} + F'\frac{\partial\bar{W}}{\partial\bar{x}} - \frac{F}{2\bar{x}}\frac{\partial\bar{W}}{\partial\eta} = \frac{1}{2\bar{x}}\frac{\partial^2\bar{W}}{\partial\eta^2}\ . \tag{2.10}$$

The appropriate boundary conditions are

$$\bar{U} = \bar{V} = \bar{W} = 0 \quad \text{at} \quad \eta = 0\ ; \quad \bar{U}\to 0, \quad \bar{W}\to \mathrm{e}^{\,\mathrm{i}\,\bar{x}} \quad \text{as} \quad \eta\to\infty. \tag{2.11}$$

In the upstream limit ($\bar{x}\to 0$), the flow becomes quasi-steady and its solution matches that of Crow (1966),

$$\bar{U}\to \tfrac{1}{2}\bar{x}\eta F''\ , \quad \bar{V}\to \tfrac{1}{4}(\eta^2 F'' - 3\eta F' - F)\ , \quad \bar{W}\to F'\ . \tag{2.12}$$

It turns out the instability of the perturbed flow at a given streamwise location is controlled by two local quantities, viz., $\bar{U}'(0,\bar{x})$ and $\bar{U}'''(0,\bar{x})$. Their variation with $\bar{x}$ is shown in Fig. 1.

2.2. *Scaling arguments*

The Klebanoff distortion in the boundary layer is concentrated in the streamwise region where $\bar{x} = O(1)$, i.e., at a distance of $l^* = O(k_1^{-1}\Lambda)$ downstream from the leading edge. Accordingly, we now introduce the Reynolds number based on l^*:

$$R = \frac{U_\infty l^*}{\nu} = R_\Lambda(\frac{l^*}{\Lambda})\ . \tag{2.13}$$

Analysis shows that the effect of Klebanoff distortion is most significant for those instability modes whose growth characteristics are controlled by the curvature of the

perturbed flow in the vicinity of the wall. A crucial observation is that, for the low-frequency (but unsteady) distortion,

$$\bar{U}'' \sim \eta \quad \text{as} \quad \eta \to 0 \ . \tag{2.14}$$

In a wall region, therefore, the Klebanoff fluctuation with suitable k_1 and ϵ_D may alter the curvature of the Blasius profile by $O(1)$, while the perturbation to the streamwise velocity itself remains small. This, in turn, can lead to fundamental changes in the nature of instability in the flow. This scenario is rather different from the case of a completely steady distortion, for which $\bar{U}'' \sim \eta^2$ as $\eta \to 0$ and, therefore, no new instability can emerge until the distortion amplitude becomes $O(1)$. Thus, there exists a crucial difference between steady and unsteady distortions, no matter how low the frequency of the unsteady distortion.

The characteristic length and time scales of the linear instability of the perturbed base flow, as well as the required strength of the distortion, is determined through a scaling argument as described below.

Consider a wall layer of thickness $\hat{\sigma}$ relative to the mean boundary-layer thickness of $R^{-\frac{1}{2}}l^*$ ($\hat{\sigma} \ll 1$). The curvature of the distortion becomes comparable with that of the Blasius profile itself when

$$\epsilon_D \hat{\sigma} (\frac{l^*}{\Lambda}) \sim \hat{\sigma}^2 \ . \tag{2.15}$$

We now seek instability waves whose streamwise wavenumbers (non-dimensionalized by $R^{\frac{1}{2}}/l^*$) are also of $O(\hat{\sigma})$.

While the growth rates of the instability modes are controlled by the distortion in the wall region, the distortion in the bulk of the flow also affects the instability wave by producing an $O(\hat{\sigma})$ correction to the phase speed and wavenumber. We will show that this correction is crucial to determining the spanwise distribution of the instability mode. The appropriate treatment can be given only when

$$\hat{\sigma}^{\frac{3}{2}} \sim \frac{R^{-\frac{1}{2}}l^*}{\Lambda} \ . \tag{2.16}$$

The exact reason for choosing the above scaling will be given in the next section.

From Eq. (2.13), Eq. (2.15) and Eq. (2.16), it follows that the streamwise wavenumber of the resultant instability waves is related to the other flow parameters via:

$$\hat{\sigma} \sim R_\Lambda^{-\frac{1}{3}} (\frac{l^*}{\Lambda})^{\frac{1}{3}} \ , \tag{2.17}$$

and that the required magnitude of the distortion is

$$\epsilon_D \sim R_\Lambda^{-\frac{1}{3}} (\frac{l^*}{\Lambda})^{-\frac{2}{3}} \ . \tag{2.18}$$

It can be shown that, for the Klebanoff distortion to induce an $O(1)$ (or larger) change in the viscous growth rate of the instability modes of interest in an unperturbed Blasius flow, we need to have $\hat{\sigma} \gg R^{-\frac{1}{20}}$. On the other hand, the foregoing analysis was based on the assumption that $\hat{\sigma} \ll 1$. These considerations impose the following restriction on the range of streamwise locations where the present analysis is formally valid:

$$R_\Lambda^{\frac{17}{23}} \ll \frac{l^*}{\Lambda} \ll R_\Lambda \ . \tag{2.19}$$

While the Klebanoff distortion modulates on the slow variables $\bar{x}$ and $\bar{t}$, instability

waves oscillate on the much faster variables $\hat{\sigma}R^{\frac{1}{2}}\bar{x}$ and $\hat{\sigma}^2R^{\frac{1}{2}}\bar{t}$. We thus introduce

$$\zeta = \hat{\sigma}R^{\frac{1}{2}}(\alpha\bar{x} - \hat{\sigma}\omega\bar{t}) \ , \tag{2.20}$$

to describe the oscillation of the carrier wave, where the scaled wavenumber α and scaled frequency ω are given via

$$\alpha = \alpha_0 + \hat{\sigma}\alpha_1 + \hat{\sigma}^2\alpha_2 \ , \quad c \equiv \omega/\alpha = c_0 + \hat{\sigma}c_1 + \hat{\sigma}c_2 + \dots \ .$$

The amplitude of the instability wave amplifies on the variable $X = \hat{\sigma}^4R^{\frac{1}{2}}\bar{x}$, which exceeds the viscous growth rate of the lower branch T-S modes when $\hat{\sigma} >> R^{-1/32}$. Since X is also much faster than $\bar{x}$ according to Eq. (2.17) and Eq. (2.19), the space and time modulation of the distortion can be treated as parametric when the stability of the perturbed flow is studied.

3. Results: intermittent instability

For the scalings identified in the previous section, the linear instability of the perturbed flow is governed by a five-zoned asymptotic structure similar to the case of a steady distortion that was analyzed in I. Unlike that distortion, however, the Klebanoff distortion in the main deck ($\hat{y} = \frac{\Lambda R^{\frac{1}{2}}}{l^*}y = (2\bar{x})^{\frac{1}{2}}\eta = O(1)$) interacts with the instability wave. This interaction has to be analyzed in order to determine the mode shape in the spanwise direction. In the main deck, the total streamwise velocity of the base flow is given by

$$U_B + \hat{\sigma}U_D(\hat{y}, Z; \bar{x}, \bar{t}) \quad \text{with} \quad U_D = -w_s'(Z)\Big(\bar{U}\,\mathrm{e}^{-\,\mathrm{i}\,\bar{t}} + c.c.\Big) \ , \tag{3.1}$$

whereas the associated fluctuation induced by the instability wave takes the form

$$u = \Big\{A(X)\Phi(Z)\hat{U}_0(\hat{y}) + \hat{\sigma}A(X)\Phi_1(Z)\hat{U}_1 + \hat{\sigma}^2\Phi_2(Z,X)\hat{U}_2 + \hat{\sigma}^3\hat{U}_3 + \dots\Big\}\,\mathrm{e}^{\mathrm{i}\,\zeta} + c.c., \tag{3.2}$$

where $A(X)$ is the amplitude of the wave. The solution in the other four decks can be sought via similar expansions. Imposing asymptotic matching requirements up to $O(\hat{\sigma}^2)$ leads to an eigenvalue problem involving the (standard) Schrödinger equation

$$-\Phi_{ZZ} = \Big(\psi(Z; \bar{x}, \bar{t}) - \alpha_s\Big)\Phi \ , \tag{3.3}$$

for the spanwise distribution of the instability mode. Here, the "potential" ψ is given by

$$\psi(Z; \bar{x}, \bar{t}) = \frac{2\lambda_D(Z)\alpha_0^2}{\lambda} = -\frac{2\alpha_0^2}{(2\bar{x})^{\frac{1}{2}}\lambda}(\bar{U}'\,\mathrm{e}^{-\,\mathrm{i}\,\bar{t}} + c.c.)w_s'(Z) \equiv -\tilde{\psi}(\bar{x}, \bar{t})w_s'(Z), \tag{3.4}$$

and α_s represents the eigenvalue parameter.

It now becomes clear that the reason for choosing Eq. (2.16) was to ensure a balance between the spanwise variation Φ_{ZZ} and the wavenumber correction $\alpha_s\Phi$ in Eq. (3.3). Without retaining Φ_{ZZ}, α_s would be parametrically dependent on the spanwise variable Z. Then the first- and second-order derivatives with respect to Z would produce secular terms proportional to $\bar{x}$ and $\bar{x}^2$, thereby invalidating the entire perturbation expansion scheme.

There is extensive literature on the Schrödinger operator. For our purpose, it suffices to mention that for a localized potential that is not negative-definite, the spectrum of the Schrödinger operator includes discrete eigenvalues with real-valued eigenfunctions that decay exponentially as $Z \to \pm\infty$. For later analysis, it is convenient to normalize the eigenfunction such that $\int_{-\infty}^{\infty}\Phi^2\,\mathrm{d}\,Z = 1$. The Schrödinger operator also has a continuous

spectrum, for which Φ remains finite and oscillatory as $Z \to \pm\infty$; however, only the discrete spectrum is considered in this paper.

The analysis can be carried to higher orders in a routine manner (cf. Wu, Stewart & Cowley 1996). The crucial equation, which determines the leading order growth rate, is obtained by considering the next, i.e., fourth term in the expansion for each deck. The final result is given by

$$-\frac{\mathrm{i}}{4\alpha_0}\Phi_{2,ZZ} = \mathrm{i}\Big\{\frac{\lambda_D(Z)\alpha_0}{2\lambda} - \alpha_s\Big\}\Phi_2 - A_X\Phi + \Big(\gamma_0 + \gamma(Z)\Big)A\Phi + \mathrm{i}\,\chi(Z,X)\ , \qquad (3.5)$$

$$\gamma_0 = -\frac{\pi c_0^4}{4\lambda} + \frac{\lambda^2}{2R^{\frac{1}{4}}\hat{\sigma}^5(2\alpha_0 c_0)^{\frac{1}{2}}}\ ,$$

$$\gamma(Z;\bar{x},\bar{t}) = -\frac{\pi c_0^3}{\lambda^2}(2\bar{x})^{-\frac{3}{2}}\Big\{\bar{U}'''(0,Z;\bar{x})\,\mathrm{e}^{-\mathrm{i}\,\bar{t}} + c.c.\Big\}w_s'(Z) \equiv -\tilde{\gamma}(\bar{x},\bar{t})w_s'(Z)\ , \qquad (3.6)$$

where χ is a real-valued function that does not affect the growth rate of the disturbance.

Equation (3.5) is an inhomogeneous Schrödinger equation. The standard procedure of imposing the solubility condition yields $A_X = (\gamma_0 + \kappa_d)A$, where

$$\kappa_d = \int_{-\infty}^{\infty} \gamma(Z)\Phi^2\,\mathrm{d}\,Z\ . \qquad (3.7)$$

The growth rate therefore corresponds to $(\gamma_0 + \kappa_d)$, κ_d being the *excess growth rate* induced by the distortion. When $\hat{\sigma} >> R^{-\frac{1}{20}}$, the excess growth rate becomes much larger than the second term in γ_0, which corresponds to the viscous contribution to the growth rate (Goldstein & Durbin 1986). In other words, the instability modes of interest are now predominantly inviscid, with a growth rate that is given by

$$\kappa = -\frac{\pi c_0^4}{4\lambda} + \int_{-\infty}^{\infty} \gamma(Z)\Phi^2\,\mathrm{d}\,Z\ . \qquad (3.8)$$

As the distortion amplitude is further increased, the inviscid growth rate continues to increase and, when $\hat{\sigma} \gg R^{-1/32}$, it exceeds the growth rate of the longer wavelength lower-branch modes which are described by the triple-deck structure and correspond to the most-unstable modes of the unperturbed flow. Clearly, the nature of the instability has been fundamentally altered at this stage.

In summary, we have seen that the asymptotic regime studied above describes a continuous transition as the distortion amplitude is varied, from a modified form of the short-wavelength, viscous modes in an unperturbed Blasius flow to primarily-inviscid modes that eventually dominate the overall instability of the perturbed flow. Because the structure of these modes can be localized in the spanwise direction and, in general, is completely dictated by the shape of the Klebanoff distortion, we will refer to these modes as *localized T-S modes*.

In order to aid our subsequent discussion, we first present solutions for the spanwise distribution $B(Z) = \frac{d^3 Z}{Z^2+d^2}$. A localized distribution of this type is believed to be appropriate to Klebanoff distortions with a finite correlation distance in Z (i.e., relative to Λ) although, of course, periodic distributions (corresponding to large coherence in Z) can also be analyzed rather easily. It follows from Eq. (2.6) that

$$-w_s'(Z) = \frac{B_0(1 - 3Z^2/d^2)}{(Z^2/d^2 + 1)^3} \equiv B_0 S(Z)\ , \quad \text{with} \quad B_0 = 2\pi\hat{v}_\infty\ . \qquad (3.9)$$

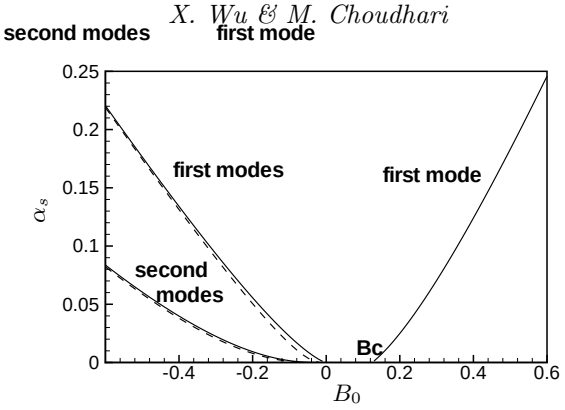

FIGURE 2. Eigenvalues α_s *v.s.* B_0: ——— varicose modes, - - - - sinuous modes.

All of the calculations presented in this paper pertain to the (arbitrary) choice of $d = 4$.

Just to illustrate the behavior of the spectrum, we first set $\tilde{\psi} = 1$ in Eq. (3.4) and plot the eigenvalues α_s for a range of B_0 (Fig. 2). Symmetric (varicose) modes can be found for both positive and negative B_0, except for the gap $0 < B_0 < 0.16 = B_c$ where they do not exist. Unlike the Schrödinger operator with a purely imaginary potential (i.e., the case analyzed in I), the standard Schrödinger equation also admits anti-symmetric (sinuous) modes in addition to the varicose ones. These modes appear only for negative B_0. For $B_0 < 0$, there also exist higher modes, symmetric or anti-symmetric, and they are distinguished by the number of zeros in the corresponding eigenfunctions. These higher modes are generally less unstable than the first ones and, accordingly, will not be discussed here any further.

Equations (3.3), (3.4) and (3.6) are used in conjunction with Eq. (3.8) to compute the inviscid growth rate due to the Klebanoff distortion. The growth rates of both the sinuous and varicose modes at three separate instants of time are shown in Fig. 3 for the case of $\bar{x} = 2.0$ and $B_0 = 1.4$. Observe that the sinuous modes have considerably larger growth rates than the varicose modes. For this reason, we shall focus on the anti-symmetric modes henceforth. Indeed, in the experiments of Matsubara & Alfredsson (2001), the sinuous modes were observed to occur more frequently.

As described earlier in the context of Fig. 2, the sinuous modes exist only when $\tilde{\psi}(\bar{x}, \bar{t})$ is negative, i.e., at those instants during the Klebanoff-mode cycle when the perturbed flow is characterized by a significant low-speed streak. This finding is consistent with most experimental observations. Furthermore, the instability occurs only in that part of cycle when $\tilde{\gamma}(\bar{x}, \bar{t})$ is also negative. On the other hand, γ and ψ tend to 0 as both $\bar{x} \to 0$ and $\bar{x} \to \infty$ (see also Fig. 1). Thus, γ and ψ have appreciable sizes over only a restricted window in the streamwise direction. The instability modes under consideration are, therefore, expected to be localized in space as well as in time.

This local and intermittent nature of the instability can be demonstrated by plotting the growth-rate contours in the $\omega - \bar{x}$ plane at various instants, as shown in Figs. 4a-d for the case of $B_0 = 1.4$. At $\bar{t} = -1.8$, a small 'bubble' of instability is observed within the $\omega - \bar{x}$ plane, indicating that the instability starts at a slightly earlier time. As time increases, the 'bubble' grows in both spatial and spectral extent, reaching its maximum at $\bar{t} \approx -0.82$, after which the 'bubble' shrinks and finally disappears, before re-emerging during the next cycle of the Klebanoff mode. Of course, given the disparity between the temporal scales of the Klebanoff mode and the instability waves, the latter

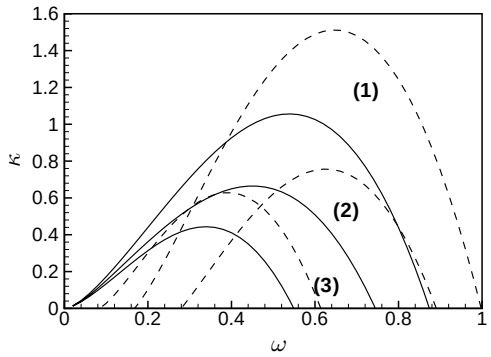

FIGURE 3. Instability caused by a Klebanoff distortion. The streamwise location is fixed at $\bar{x} = 2.0$ and $B_0 = 1.4$. The Figure shows the growth rates of varicose (————) and sinuous modes (– – – –) at three instants: (1) $\bar{t} = \phi(\bar{x}) - \frac{3}{4}\pi$; (2) $\bar{t} = \phi(\bar{x}) - \frac{7}{8}\pi$; (3) $\bar{t} = \phi(\bar{x}) - \frac{29}{32}\pi$.

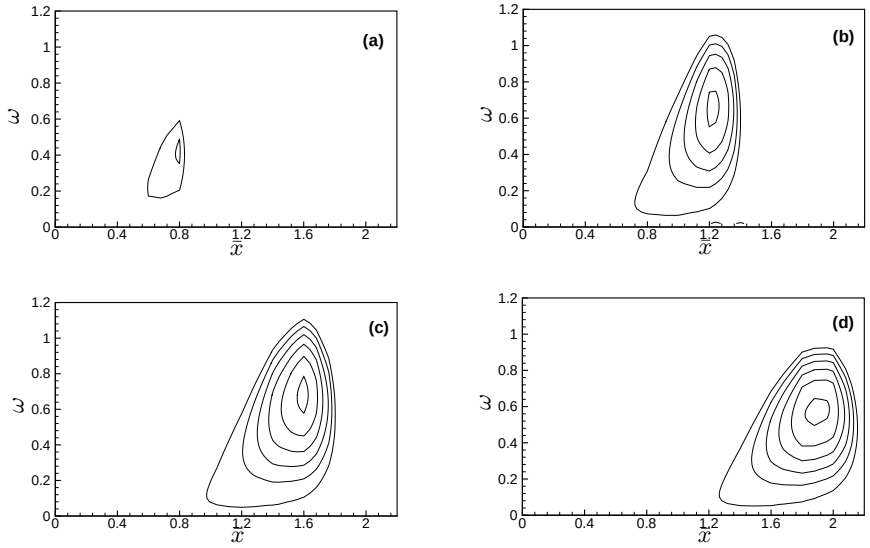

FIGURE 4. Contours of growth rates of the local instability induced by a Klebanoff mode ($B_0 = 1.4$). Figures (a)-(d) correspond to the instants $\bar{t} = -1.8, -1.25, -0.82, -0.44$.

could amplify substantially within a single period of modulation and, therefore, reach sufficiently high amplitudes to induce a local breakdown. In reality, the modulation is stochastic so that this local instability takes place randomly as, indeed, has been observed in the experiments of Kendall (1985).

From Figs. 4a-d, one may deduce useful information about the spatio-temporal behaviour of the instability. The localized structure of the instability wave in both x and Z suggests that the unstable modes would be manifested as patches of oscillations. Strictly speaking, the center of these patches can only be determined after considering the complex history of the disturbance motion. However, it may still be useful to model the center of a patch as being close to the $\bar{x}$ location that corresponds to the growth rate maximum in Figs. 4a-d. From $\bar{t} = -1.80$ to $\bar{t} = -0.82$, the center of the patch migrates from $\bar{x} = 0.8$ to 1.6, yielding an apparent patch *convection velocity* of $V_c \approx 0.82$. Though

this prediction is based on a number of simplifying assumptions, migration of patches at such a speed appears to have been observed in experiments as well.

4. Discussions and conclusions

In this paper, we have investigated the effect of long-wavelength Klebanoff fluctuations on the instability of the Blasius boundary layer. By using an asymptotic approach based on the high-Reynolds-number assumption, we have derived a self-consistent, albeit simplified, mathematical model, which appears to capture certain key elements of this problem. Specifically, our analysis indicates that relatively weak Klebanoff fluctuations, which do not alter the velocity profile by $O(1)$, may change the near-wall curvature of the underlying Blasius flow by $O(1)$. This, in turn, has the effect of modifying and even fundamentally altering the instability of the boundary-layer flow. Specifically, a localized distortion may induce both sinuous and varicose modes of instability. However, the sinuous modes are found to be more unstable, in general.

When the distortion is just strong enough to produce an excess growth comparable to viscous growth, these modes may be viewed as modified T-S waves. However as the strength of the distortion exceeds a threshold range (in an asymptotic sense), the instability becomes essentially inviscid, and the characteristic frequencies and growth rates are now much higher than those of the T-S waves in an unmodified Blasius flow. Because the Klebanoff distortion modulates the base flow in both t and x, its effect on the instability is intermittent in time and localized in space, i.e., it is manifested only during a certain phase of the modulation and in a limited window along the streamwise direction. In particular, the dominant sinuous modes appear during the phase in which the flow is characterised by low-speed streaks.

An interesting feature of the instability modes analyzed in this paper is that, despite the low-frequency nature of the Klebanoff distortion, the unsteadiness of the latter plays a crucial role in this model. Specifically, the above instability modes would not have been predicted for a small-amplitude Klebanoff distortion if it had been treated as being steady. Moreover, the intermittent nature and the convection of unstable patches or spots are both attributable to the unsteadiness of the distortion.

The qualitative predictions of our theory are consistent with laboratory observations. Our results indicate that the streaks can become unstable even without appreciable changes in the Blasius profile. This is precisely what Matsubara *et al.* (2000) concluded on the basis of their experimental studies. The predicted patches of oscillations have been observed in numerous experiments. The elevated growth of instability wave packets in the presence of Klebanoff distortion has also been observed in the experiments by Kendall (1991), as mentioned in the Introduction.

The seemingly puzzling and conflicting experimental observations can be reconciled to some degree when reinterpreted in the light of our theoretical results. As mentioned in §1, the wavepackets develop out of the background disturbance and amplify downstream. Kendall (1990) associated these with T-S waves. We believe that they are likely to be packets of the local T-S waves identified in this paper, rather than the usual T-S waves in an unmodified Blasius flow. These local T-S waves exhibit virtually all of the unusual characteristics observed by Kendall: the onset threshold, the excess growth, and the range of higher frequencies. Since their growth rates depend on the magnitude of the Klebanoff fluctuation, it is to be expected that their amplitude at a particular observation point should have a nonlinear relation with the magnitude of the Klebanoff motion. Since the

spanwise extent of these local T-S modes is determined by the Klebanoff distortion, it is not surprising that they undergo little lateral spreading.

The extreme sensitivity of the boundary-layer response to harmonic point excitation (Watmuff 1997, 1998) can also be explained. In the presence of Klebanoff fluctuations, a point excitation definitely generates local T-S modes as well. Therefore, the general response cannot be represented as a summation of the conventional T-S waves, as was done in the calculation. This may be the reason why a meaningful comparison is not possible unless the Klebanoff fluctuation is substantially reduced.

Jacobs & Durbin (2001) concluded from their direct numerical simulations of bypass transition that the streaks close to the wall are stable. Our results seem to be in conflict with this finding. There could be a number of reasons for the disagreement. It might be that the present instability is so weak that it is masked by other more vigorous processes. Alternatively, it is plausible that the instability modes identified herein were not excited in their simulations. Finally, the energy of the free-stream disturbances in their simulation is contained in a band of rather high frequencies (an order-of-magnitude higher than typical frequencies of T-S waves) and, therefore, the streaks are not a linear response to the low-frequency components. Rather, they are generated nonlinearly by the interaction of higher-frequency components. The question as to whether or not this is the cause of the discrepancy remains open at this point.

The present work is, of course, far from being a complete or quantitatively accurate description of the problem. The primary shortcoming is its neglect of the spanwise ellipticity of the Klebanoff fluctuation. The more general problem for Klebanoff distortions with an $O(1)$ wavelength, including the effects of nonlinearity and stochasticity, is currently under investigation. Nonetheless, the simplicity of the current model, together with the physical insights derived from it, appear to justify the assumptions made herein. The theory, we believe, sheds useful light on a very complex process which has so far eluded a first-principles explanation.

The work of XW was carried out during his sabbatical in 2001 at ICASE NASA Langley and the Center for Turbulence Research. He would like to thank Professors Parviz Moin, Paul Durbin, W. C. Reynolds and Peter Bradshaw for helpful discussions and comments.

REFERENCES

Andersson, P., Brandt, L., Bottaro, A. & Henningson, D. S. 2001 On breakdown of boundary layer streaks. *J. Fluid Mech.* **428**, 29-60.

Arnal, D. & Juillen, J .C. 1978 Contribution expérimental a l'étude de la réceptivité d'une couche limite laminaire, à la turbulence de l'écoulement général. *ONERA Tech.* No. 1/5018 AYD.

Choudhari, M. 1996 Boundary-layer receptivity to three-dimensional unsteady vortical disturbances in free stream. *AIAA* Paper 96-0181.

Crow, S. C. 1966 The spanwise perturbation of two-dimensional boundary layers. *J. Fluid Mech.* **24**, 153-164.

Dryden, H. L. 1936 Air flow in the boundary layer near a plate. *NACA* Report 562.

Goldstein, M. E. & Durbin, P. A. 1986 Nonlinear critical layers eliminate the upper branch of spatially growing Tollmien-Schlichting waves. *Phys. Fluids* **29**, 2334-2345.

Goldstein, M. E. & Wundrow, D. W. 1998 On the environmental realizability of algebraically growing disturbances and their relation to Klebanoff modes. *Theo. Comp. Fluid Dyn.* **10**, 171-186.

Gulyaev, A. N., Kozlov, V., Kuznetsov, V. R., Mineev, B. I. & Sekundov, A. N. 1989 Interaction of laminar boundary layer with external turbulence. *Izv. Akad. Nauk SSSR Mekh. Zhid. Gaza* **6**, 700-710.

Kendall, J. M. 1985 Experimental study of disturbances produced in pre-transitional laminar boundary layer by weak free stream turbulence. *AIAA* Paper 85-1695.

Kendall, J. M. 1990 Boundary-layer receptivity to free-stream turbulence. *AIAA* Paper 80-1504.

Kendall, J. M. 1991 Studies on laminar boundary layer receptivity to freestream turbulence near a leading-edge. In *Boundary Layer Stability and Transition to Turbulence* (D. C. Reda, R. H. Reed & R. Kobayashi, eds.). ASME FED, **114**, 23-30.

Kendall, J. M. 1998 Experiments on boundary-layer receptivity to freestream turbulence. *AIAA* Paper 98-0530.

Klebanoff, P. S. 1971 Effect of free-stream turbulence on a laminar boundary layer. *Bulletin. Am. Phys. Soc.* **16**.

Jacobs, R. G. & Durbin, P. A. 2001 Simulations of bypass transition. *J. Fluid Mech.* **428**, 185-212.

Leib, S. J., Wundrow, D. W. & Goldstein, M. E. 1999 Effect of free-stream turbulence and other vortical disturbances on a laminar boundary layer. *J. Fluid Mech.* **380**, 169-203.

Matsubara M., Bakchinov A. & Alfredsson, P. H. 2000 In *Proc. IUTAM Symposium on Laminar-Turbulent Transition* (H. Fasel & W. Saric, eds.). Springer.

Matsubara, M. & Alfredsson, P. H. 2001 Disturbance growth in boundary layers subjected to free-stream turbulence. *J. Fluid Mech.* **430**, 149-168.

Rai, M. M. & Moin, P. 1993 Direct numerical simulation of transition and turbulence in a spatially evolving boundary layer. *J. Comput. Phys.* **109**, 169-192.

Schlichting, H. 1933 Zur Entstehung der Turbulenz bei der Plattenstromung. *Nachr. Ges. Wiss. Göttingen Math.-Phys. Kl. 1933*, 181-208.

Taylor, G. I. 1939 Some recent developments in the study of turbulence. In *Proc. 5th Intl. Congr. Appl. Mech.* (J. P. Den Hartog & H. Peters, eds.). Wiley, 294-310.

Tollmien, W. 1929 Über die Entstehung der Turbulenz. *Nachr. Ges. Wiss. Göttingen Math.-Phys. Kl. 1929*, 21-44.

Watmuff, J. H. 1997 Interactions between Klebanoff modes and TS waves in a Blasius boundary layer. *AIAA* Paper 97-0558.

Watmuff, J. H. 1998 Detrimental effects of almost immeasurably small freestream nonuniformities generated by wind-tunnel screens. *AIAA J.* **36**, 379-386.

Westin, K. J., Boiko, A. V., Klingmann, B. G. B., Kozlov, V. V. & Alfredsson, P. H. 1994 Experiments in a boundary layer subjected to free stream turbulence. Part I. Boundary layer structure and receptivity. *J. Fluid Mech.* **281**, 193-218.

Wu, X., Stewart, P. A. & Cowley, S. J. 1996 On the weakly nonlinear development of Tollmien-Schlichting wave-trains in boundary layers. *J. Fluid Mech.* **316**, 133-171.

Wu, X. & Luo, J. 2001 Instability of Blasius boundary layer in the presence of steady streaks. *Annual Research Briefs*, Center for Turbulence Research, NASA Ames/Stanford Univ., 293–304.

Wundrow, D. W. & Goldstein, M. E. 2001 Effect on a laminar boundary layer of small-amplitude streamwise vorticity in the upstream flow. *J. Fluid Mech.* **426**, 229-262.